Cell Reports Physical Science, Volume *3*

Supplemental information

Mechanosensing view of SARS-CoV-2 infection by a DNA nano-assembly

Jialu Zhang, Yihao Huang, Miao Sun, Ting Song, Shuang Wan, Chaoyong Yang, and Yanling Song

Supporting Information

Supporting Figures

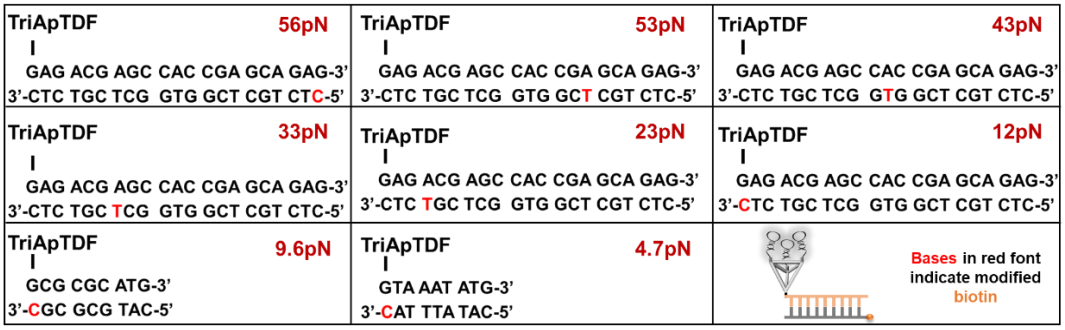

Figure S1. The TGT module comprising double-stranded DNA in unzipping or shear geometry, displaying estimated tensile forces of 4.7, 9.6, 12, 23, 33, 43 and 56 pN[1,2]. Using DNA hybridization, we obtained a series of TGT modules with different defined pN-scale tensile forces.

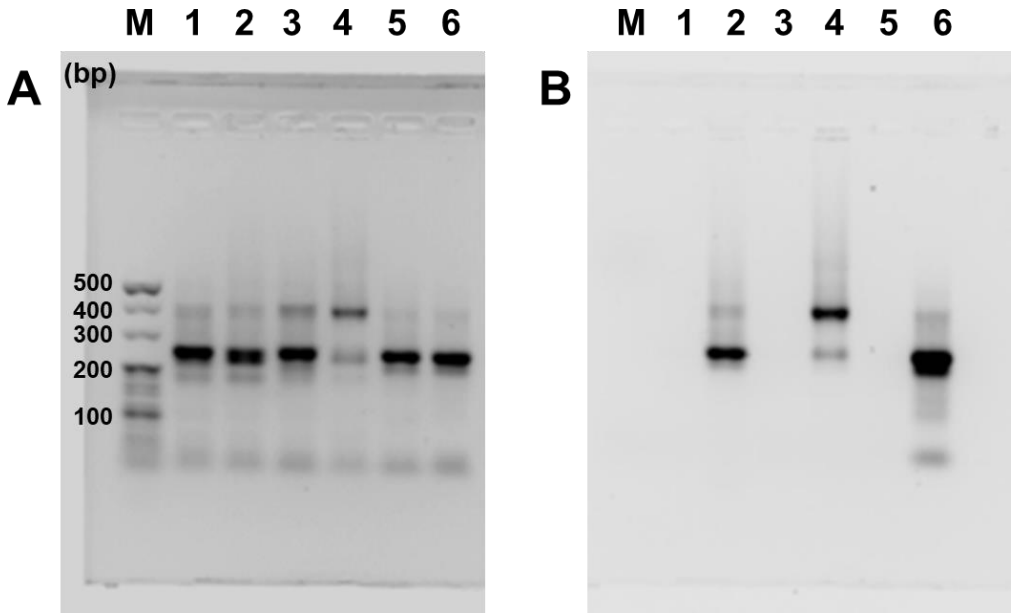

Figure S2. Agarose gel electrophoresis analysis of the binding module at excitation wavelength of (A) UV and (B) 647 nm. Lane 1: s12-56pN-TriApTDF, Lane 2: Cy5-labelled s12-56pN-TriApTDF, Lane 3: s9.6pN-TriApTDF, Lane 4: Cy5-labelled s9.6pN-TriApTDF, Lane 5: s4.7pN-TriApTDF and Lane 6: Cy5 labelled s4.7pN-TriApTDF. Although Cy5-labelled s9.6pN-TriApTDF displayed many more by-products, we mainly used s4.7pN-TriApTDF, s9.6pN-TriApTDF and s12-56pN-TriApTDF to analyze the mechanical force between SARS-CoV-2 and host cell. The extra band below 100 bp may be the excess single-stranded DNA of A17-12-56pN, or A17-9.6pN, or A17-4.7pN.

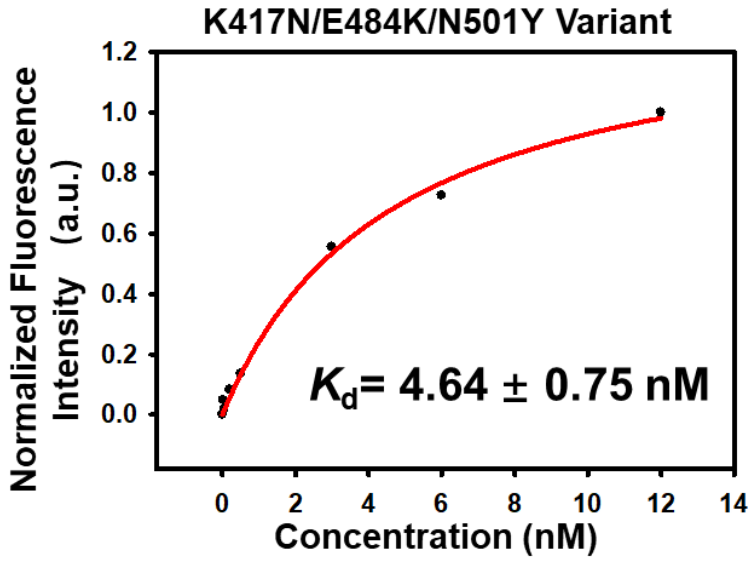

Figure S3. The binding curve and dissociation constant of TriApTDF against SARS-CoV-2 RBD-beads of K417N/E484K/N501Y variant in binding buffer.

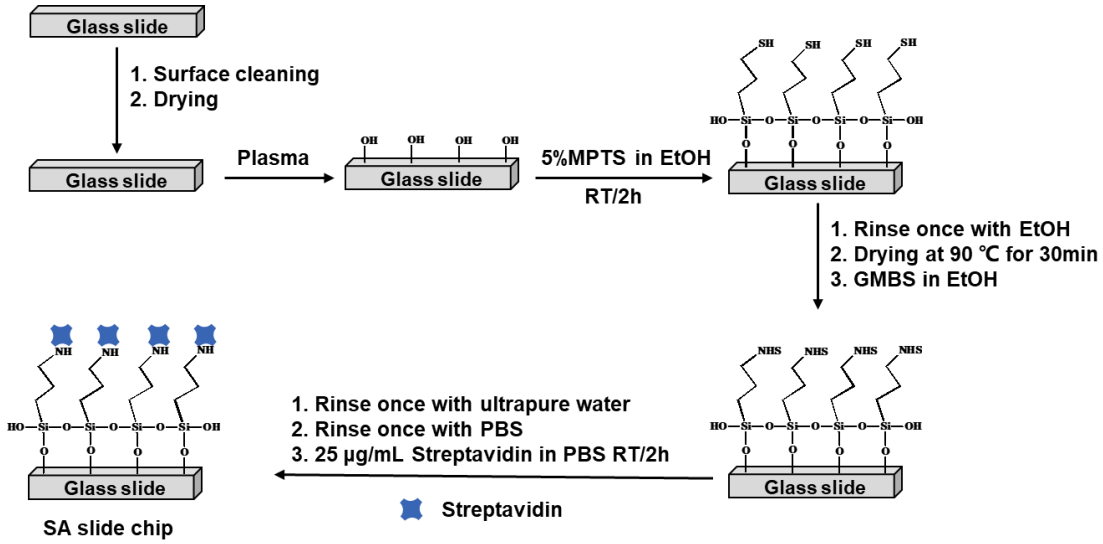

Figure S4. Diagram of the modification process for streptavidin-functionalized glass slide chip.

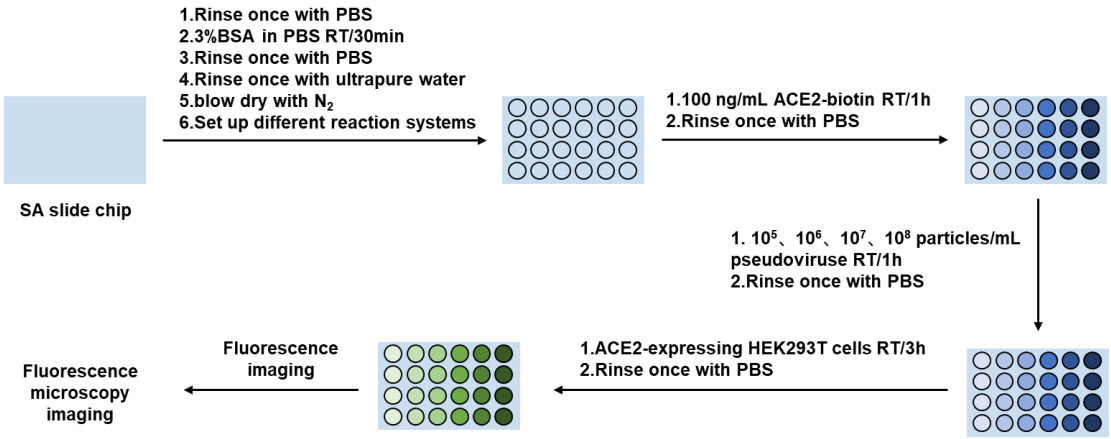

Figure S5. Experimental process of the optimization of the particle concentration of wild type SARS-CoV-2 pseudoviruses.

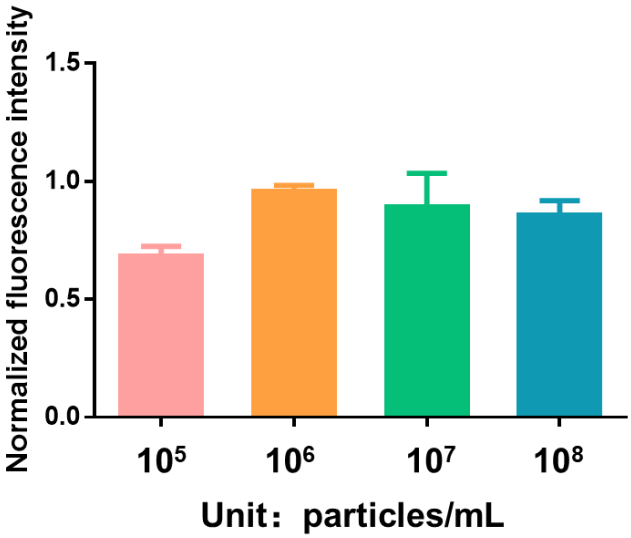

Figure S6. The optimization of the particle concentration of wild type SARS-CoV-2 pseudoviruse.

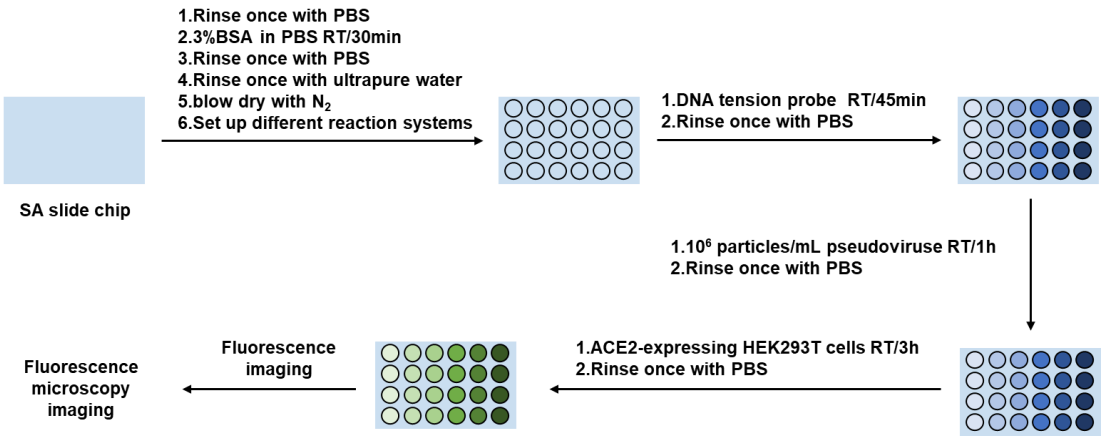

Figure S7. Working flow chart of Virus-TGT for determining the mechanical forces between SARS-CoV-2 pseudovirus and ACE2-expressing HEK293T cells.

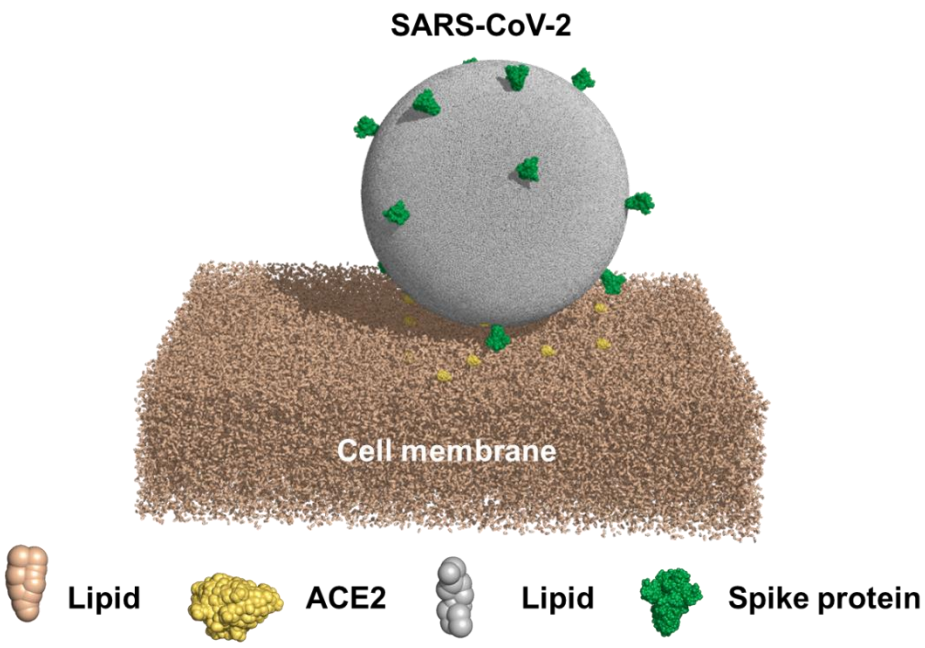

Figure S8. Schematic illustration of the CG model in DPD simulations: SARS-CoV-2 virus nanoparticle (90 nm) consists of twelve spike trimer protein. Spike protein with green color represents wild type SARS-CoV-2 virus based on the protein crystal structures of wild type (PDB: 7DDN). The cell membrane is composed of lipids (light brown) and membrane protein ACE2 (yellow).

Supporting Tables

Table S1. DNA sequences.

Name	Sequence (5'-3')
A17-12-56pN	ACATTCCTAAGTCTGAAACATTACAGCTTGCTACACGAGAAGAGCCGCCATAGTATTGAGACGAGCCACCGAGCAGAG
A17-12-56pN-cy5	ACATTCCTAAGTCTGAAACATTACAGCTTGCTACACGAGAAGAGCCGCCATAGTATTGAGACGAGCCACCGAGCAGAG-cy5
A17-9.6pN	ACATTCCTAAGTCTGAAACATTACAGCTTGCTACACGAGAAGAGCCGCCATAGTATTGCGCGCATG
A17-9.6pN-cy5	ACATTCCTAAGTCTGAAACATTACAGCTTGCTACACGAGAAGAGCCGCCATAGTATTGCGCGCATG-cy5
A17-4.7pN	ACATTCCTAAGTCTGAAACATTACAGCTTGCTACACGAGAAGAGCCGCCATAGTATTGTAAATATG
A17-4.7pN-cy5	ACATTCCTAAGTCTGAAACATTACAGCTTGCTACACGAGAAGAGCCGCCATAGTATTGTAAATATG-cy5
A	ACATTCCTAAGTCTGAAACATTACAGCTTGCTACACGAGAAGAGCCGCCATAGTA
B17-L	TATCACCAGGCAGTTGACAGTGTAGCAAGCTGTAATAGATGCGAGGGTCCAATACCTGACCACGAGCTCC
C17-L	TCAACTGCCTGGTGATAAAACGACACTACGTGGGAATCTACTATGGCGGCTCTTCCTGACCACGAGCTCC
D17-L	TTCAGACTTAGGAATGTGCTTCCCACGTAGTGTCGTTTGTATTGGACCCTCGCATCTGACCACGAGCTCC
B17	TATCACCAGGCAGTTGACAGTGTAGCAAGCTGTAATAGATGCGAGGGTCCAATAC
C17	TCAACTGCCTGGTGATAAAACGACACTACGTGGGAATCTACTATGGCGGCTCTTC
D17	TTCAGACTTAGGAATGTGCTTCCCACGTAGTGTCGTTTGTATTGGACCCTCGCAT
CoV2-6C-L	CGCAGCACCCAAGAACAAGGACTGCTTAGGATTGCGATAGGTTCGGGGAGCTCGTGGTCAG
Alexa 488-CoV2-6C-L	Alexa 488-CGCAGCACCCAAGAACAAGGACTGCTTAGGATTGCGATAGGTTCGGGGAGCTCGTGGTCAG
cy5-CoV2-6C-L	cy5-CGCAGCACCCAAGAACAAGGACTGCTTAGGATTGCGATAGGTTCGGGGAGCTCGTGGTCAG
56pN	CTCTGCTCGGTGGCTCGTCTC
53pN	CTCTGCTCGGTGGCTCGTCTC
43pN	CTCTGCTCGGTGGCTCGTCTC
33pN	CTCTGCTCGGTGGCTCGTCTC
23pN	CTCTGCTCGGTGGCTCGTCTC
12pN	CTCTGCTCGGTGGCTCGTCTC
9.6pN	CATGCGCGC
4.7pN	CATATTTAC

Table S2. DNA sequences for corresponding experiments.

Number	Probe Name	DNA sequence involved	Experiment name
1	s12-56pN-TDF	A17-12-56pN, B17, C17, D17	Agarose gel electrophoresis analysis
2	s12-56pN-LTDF	A17-12-56pN, B17-L, C17, D17	
3	s12-56pN-DimTDF	A17-12-56pN, B17-L, C17-L, D17	
4	s12-56pN-TriTDF	A17-12-56pN, B17-L, C17-L, D17-L	
5	s12-56pN-ApTDF	A17-12-56pN, B17-L, C17, D17, CoV2-6C-L	
6	s12-56pN-DimApTDF	A17-12-56pN, B17-L, C17-L, D17, CoV2-6C-L	
7	s12-56pN-TriApTDF(cy5)	A17-12-56pN(-cy5), B17-L, C17-L, D17-L, CoV2-6C-L	
8	s9.6pN-TriApTDF(cy5)	A17-9.6pN(-cy5), B17-L, C17-L, D17-L, CoV2-6C-L	
9	s4.7pN-TriApTDF(cy5)	A17-4.7pN(-cy5), B17-L, C17-L, D17-L, CoV2-6C-L	
10	s12-56pN-TriApTDF	A17-12-56pN, B17-L, C17-L, D17-L, CoV2-6C-L	Cryo-EM
11	TriApTDF (Alexa 488)	A17, B17-L, C17, D17, Alexa 488-CoV2-6C-L	Flow cytometry analysis
12	s12-56pN-DimApTDF (Alexa 488:cy5=1:1)	A17-12-56pN, B17-L, C17-L, D17, Alexa 488-CoV2-6C-L, cy5-CoV2-6C-L	Total internal reflection fluorescent microscope
13	s12-56pN-TriApTDF (Alexa 488:cy5=2:1)	A17-12-56pN, B17-L, C17-L, D17-L, Alexa 488-CoV2-6C-L, cy5-CoV2-6C-L	
14	56pN-TriApTDF (cy5)	A17-12-56pN-cy5, B17-L, C17-L, D17-L, CoV2-6C-L, 56pN	Fluorescence microscope
15	4.7pN-TriApTDF (cy5)	A17-4.7pN-cy5, B17-L, C17-L, D17-L, CoV2-6C-L, 4.7pN	
16	12-56pN-TriApTDF	12-56pN-TriApTDF, 12pN or 23pN or 33pN or 43pN or 53pN or 56pN	Virus-TGT measurement
17	9.6pN-TriApTDF	A17-9.6pN, B17-L, C17-L, D17-L, CoV2-6C-L, 9.6pN	
18	4.7pN-TriApTDF	A17-4.7pN, B17-L, C17-L, D17-L, CoV2-6C-L, 4.7pN	

Table S3. Comparison of previous SARS-CoV-2 virus-related studies to Virus-TGT in this work.

Title	Measurement object	Method	Journal
Multivalent 9-O-Acetylated-sialic acid glycoclusters as potent inhibitors for SARS-CoV-2 infection[3]	SARS-CoV-2/S1 and ACE2	single molecule atomic force microscopy	***Nat. Commun.*** 2022, 13 (1), 2564.
N501Y mutation of spike protein in SARS-CoV-2 strengthens its binding to receptor ACE2[4]	RBD and ACE2-expressing cell	single molecule atomic force microscopy	***eLife*** 2021, 10, e69091.
Molecular interaction and inhibition of SARS-CoV-2 binding to the ACE2 receptor[5]	S1/RBD and ACE2	single molecule atomic force microscopy	***Nat. Commun.*** 2020, 11 (1), 4541.
Molecular insights into receptor binding energetics and neutralization of SARS-CoV-2 variants[6]	RBD and ACE2	single molecule atomic force microscopy	***Nat. Commun.*** 2021, 12 (1), 6977.
Biomechanical characterization of SARS-CoV-2 spike RBD and human ACE2 protein-protein interaction[7]	RBD and ACE2	single molecule atomic force microscopy	***Biophys. J.*** 2021, 120 (6), 1011-1019.
Mechanical activation of spike fosters SARS-CoV-2 viral infection[8]	Spike/RBD and ACE2	single-molecule magnetic tweezers	***Cell Res.*** 2021, 31 (10), 1047-1060.
A tethered ligand assay to probe SARS-CoV-2: ACE2 interactions[9]	RBD and ACE2	single-molecule magnetic tweezers	***Proc. Natl Acad. Sci. USA*** 2022, 119 (14), e2114397119.

References

1. Wang, X., and Ha, T. (2013). Defining single molecular forces required to activate integrin and notch signaling. Science *340*, 991-994. 10.1126/science.1231041.

2. Yin, F., Li, M., Mao, X., Li, F., Xiang, X., Li, Q., Wang, L., Zuo, X., Fan, C., and Zhu, Y. (2020). DNA Framework-Based Topological Cell Sorters. Angew. Chem. Int. Ed. *59*, 10406-10410. 10.1002/anie.202002020.

3. Petitjean, S.J.L., Chen, W., Koehler, M., Jimmidi, R., Yang, J., Mohammed, D., Juniku, B., Stanifer, M.L., Boulant, S., Vincent, S.P., et al. (2022). Multivalent 9-O-Acetylated-sialic acid glycoclusters as potent inhibitors for SARS-CoV-2 infection. Nat. Commun. *13*, 2564. 10.1038/s41467-022-30313-8.

4. Tian F, Tong B, Sun L, Shi S, Zheng B, Wang Z, Dong X, and P., Z. (2021). N501Y mutation of spike protein in SARS-CoV-2 strengthens its binding to receptor ACE2. eLife *10*, e69091. 10.7554/eLife.69091.

5. Yang, J., Petitjean, S.J.L., Koehler, M., Zhang, Q., Dumitru, A.C., Chen, W., Derclaye, S., Vincent, S.P., Soumillion, P., and Alsteens, D. (2020). Molecular interaction and inhibition of SARS-CoV-2 binding to the ACE2 receptor. Nat. Commun. *11*, 4541. 10.1038/s41467-020-18319-6.

6. Koehler, M., Ray, A., Moreira, R.A., Juniku, B., Poma, A.B., and Alsteens, D. (2021). Molecular insights into receptor binding energetics and neutralization of SARS-CoV-2 variants. Nat. Commun. *12*, 6977. 10.1038/s41467-021-27325-1.

7. Cao, W., Dong, C., Kim, S., Hou, D., Tai, W., Du, L., Im, W., and Zhang, X.F. (2021). Biomechanical characterization of SARS-CoV-2 spike RBD and human ACE2 protein-protein interaction. Biophys. J. *120*, 1011-1019. 10.1016/j.bpj.2021.02.007.

8. Hu, W., Zhang, Y., Fei, P., Zhang, T., Yao, D., Gao, Y., Liu, J., Chen, H., Lu, Q., Mudianto, T., et al. (2021). Mechanical activation of spike fosters SARS-CoV-2 viral infection. Cell Res. *31*, 1047-1060. 10.1038/s41422-021-00558-x.

9. Bauer, M.S., Gruber, S., Hausch, A., Gomes, P., Milles, L.F., Nicolaus, T., Schendel, L.C., Navajas, P.L., Procko, E., Lietha, D., et al. (2022). A tethered ligand assay to probe SARS-CoV-2:ACE2 interactions. Proc. Natl Acad. Sci. USA *119*, e2114397119. 10.1073/pnas.2114397119.